

promoting access to White Rose research papers



Universities of Leeds, Sheffield and York
<http://eprints.whiterose.ac.uk/>

This is an author produced version of a paper published in **Physica Status Solidi. Rapid Research Letters**.

White Rose Research Online URL for this paper:
<http://eprints.whiterose.ac.uk/43727/>

Published paper

Morley, SA, Porter, NA and Marrows, CH (2011) *Magnetism and magnetotransport in sputtered Co-doped FeSi films*. Physica Status Solidi. Rapid Research Letters, 5 (12). 429 - 431

<http://dx.doi/10.1002/pssr.201105386>

Magnetism and magnetotransport in sputtered Co-doped FeSi films

Sophie A. Morley¹, Nicholas A. Porter¹, and Christopher H. Marrows^{*, 1}

¹ School of Physics and Astronomy, University of Leeds, Leeds LS2 9JT, United Kingdom

Received XXXX, revised XXXX, accepted XXXX

Published online XXXX

Key words: Transition metal monosilicide, linear magnetoresistance, anomalous Hall effect, half-metal

* Corresponding author: e-mail c.h.marrows@leeds.ac.uk, Phone: +44-113-3433780, Fax: +44-113-3433900

FeSi is a non-magnetic narrow-gap semiconductor that can be doped *n*-type by Co, which also gives rise to magnetic order. Here we report on the growth of sputtered thin films of Fe_{0.8}Co_{0.2}Si, which are predominantly ϵ -phase (B20 lattice structure), and possess that phase's characteristic magnetotransport properties.

The ordinary Hall coefficient shows that each Co atom donates roughly one electron, whilst the magnetometry suggests that each gives rise to close to one Bohr magneton of moment. These results indicate that a highly spin-polarised electron gas persists despite the inevitable disorder in these thin films, suitable for spintronic devices.

Copyright line will be provided by the publisher

1 Introduction Fe_{1-x}Co_xSi is a remarkable compound which has attracted much attention due to its unusual magnetic and electrical properties. At room temperature, the parent FeSi compound takes its most stable crystal structure, the cubic B20 or ϵ -phase [1]. This non-magnetic phase has a low carrier density and is a strongly-correlated narrow-gap insulator at low temperatures [2]. Conventional band theory does not adequately explain the remarkable thermodynamic behaviour of FeSi [3, 4]; it has been suggested it can be described by spin fluctuations or as a *d*-electron Kondo insulator [5]. However, recent findings using photoemission spectroscopy argue it is most appropriately described as an itinerant semiconductor [6, 7].

Manyala *et al.* have shown that the conductivity of FeSi increases on Co doping [8]; they report that substituting Co for Fe gives rise to electron-doping and that each Co atom contributes one Bohr magneton (μ_B) to the spontaneous magnetisation in a high-quality bulk crystal [9]. Local-density approximation calculations for the band structure have been computed by Guevara *et al.* [10], and have shown that the ϵ -phase of the doped material has a half-metallic ground state. The prospect of a highly-spin polarised material based on Si is very attractive for spintronics applications [11]. Nevertheless, to realise its technological potential, thin films are needed.

In the past, thin film growth of FeSi has been carried out using molecular beam epitaxy (MBE) techniques

[12] or pulsed laser ablation [13]. Thin film growth of the Co-doped material has been documented for variable doping ranges, using pulsed laser deposition (PLD) techniques [14]. These methods produce highly ordered films, in contrast to the polycrystalline material that typically arises from sputtering. Despite this, the thin films grown here, although possessing some disorder, still exhibit the unusual properties that have only previously been studied in high quality, single crystal bulk samples [8, 9, 15].

2 Methods Samples were sputtered from a stoichiometric Fe_{0.8}Co_{0.2}Si target onto MgO (001) substrates in a chamber with a base pressure of $\sim 2 \times 10^{-8}$ Torr. The rate of deposition was $\sim 0.3 \text{ \AA s}^{-1}$, as determined by x-ray reflectometry. The samples were annealed post-growth in a two step process; firstly, a 15 °C/min ramp to a 30 minute hold at 250 °C to outgas the vacuum furnace, followed by a similar ramp to 600 °C for a 120 minute hold.

Vibrating sample magnetometry (VSM) was used to obtain the magnetic data with the field applied in the plane of a 43 ± 1 nm thick sheet film. Standard four-probe longitudinal and Hall resistivity measurements were made on a Hall bar geometry sample (47 ± 1 nm thick) defined by depositing through a shadow mask. The measurements were carried out in a gas-flow cryostat with the field applied normal to the sample plane. An ~ 80 nm thick cross-section for high-resolution transmission electron mi-

Copyright line will be provided by the publisher

croscopy (HRTEM) and energy dispersive x-ray analysis (EDX) was prepared using a focussed ion beam (FIB) on this sample subsequent to measurement.

3 Results and discussion

3.1 Structural characterisation A TEM image of part of this FIB cross-section is shown in Fig. 1(a). An amorphous layer of silica (composition confirmed by EDX), 3–4 nm thick, can be seen as a bright stripe at the top and bottom of the film, probably formed during annealing. The FeCoSi film is not laterally homogeneous: some parts (10–15% of the film) appear darker than the rest. HRTEM images of the regions between these dark parts show lattice fringes that extend throughout the film height, displayed in Fig. 1(b) and its inset. This is consistent with a Scherrer analysis of the narrow B20-structure Bragg peaks seen in X-ray diffraction patterns of a sheet film (not shown), which indicates crystallographic coherence over lengthscales comparable with the film thickness. The lattice constant measured from an FFT in these areas, calibrated against that of the MgO substrate, is 4.45 ± 0.04 Å, in keeping with expectation for the Co-doped material. Selected area K-edge EDX here with a ~ 5 nm probe yields a stoichiometry of $\text{Fe}_{0.80}\text{Co}_{0.20}\text{Si}_{1.17}$, slightly Si-rich but at the nominal Co doping level. The dark regions show nanocrystallinity with some amorphous parts, displayed in Fig. 1(c) and its inset, so are difficult to assign to any specific phase. The stoichiometry within this region yields $\text{Fe}_{0.88}\text{Co}_{0.11}\text{Si}_{0.58}$: slightly underdoped with Co but very Si deficient, the Si presumably having migrated to form the SiO_x layers during annealing.

3.2 Magnetic characterisation Hysteresis loops measured by VSM are shown inset to Fig. 2(a). Loops measured above $T \sim 40$ K show a ferromagnetic response that is largely temperature independent, which we attribute to the Fe and Co-rich non-B20 phase material, which will have a high Curie temperature. There is also a more slowly saturating contribution that first appears at the ϵ -phase Curie temperature $T_C \sim 40$ K [9], and grows as the sample is cooled further, which we attribute to the ϵ -phase material. In Fig. 2(a) we show the size of the latter contribution in units of μ_B per Co atom at 1 T, having subtracted temperature-independent background. It reaches $\sim 1\mu_B/\text{Co}$ at low temperatures.

3.3 Magnetotransport The temperature dependence of the resistivity of ϵ -phase $\text{Fe}_{1-x}\text{Co}_x\text{Si}$ has a characteristic form that reflects its electronic band structure [9, 15]. Fig. 2(b) shows that it is well-reproduced in our sample. Furthermore, the absolute resistivities are very similar to those measured for well-ordered single crystals [15]. On application of an 8 T field we see that there is significant magnetoresistance below ~ 60 K, of comparable magnitude to that found in bulk crystals [9, 15], or chemically synthesised nanowires [16]. In the inset of Fig. 2(b) we show the magnetoresistance isotherms at various temperatures below this value. All show positive linear mag-

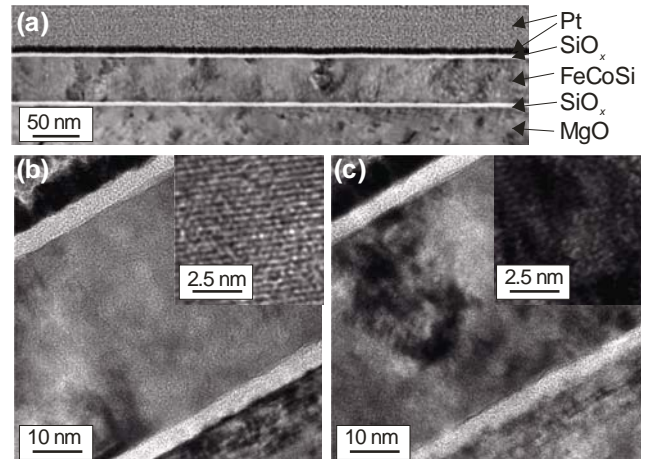


Figure 1 TEM characterisation. (a) Survey image, with the various layers marked, including the Pt cap added for FIB sample preparation. The dark band is sputtered Pt, above it is e-beam evaporated Pt. (b) HRTEM image of a ϵ -phase pure part of the film. (c) HRTEM image including a Si-deficient region, which appears darker than the surrounding B20 material. Insets to (b) and (c) show higher magnifications of relevant areas.

netoresistance to very low fields, explained by Manyala *et al.* as being due to quantum interference phenomena [9]. What is particularly striking about the transport data is that they are very similar to those found for phase-pure B20 single crystals in spite of the much higher level of disorder in our sputtered films, indicating that the ϵ -phase material is dominating.

We also measured the Hall resistivity of our sample. For $T \lesssim T_C$ K we find a strong anomalous Hall contribution, in addition to the ordinary Hall effect, defined as the Hall resistance obtained when the high-field ordinary Hall slope is extrapolated back to zero field. We plot this signal in Fig. 2(a) and can see that it resembles the magnetisation of the sheet film as measured by VSM.

We used the ordinary Hall slope, measured at high fields (>5 T), to determine the carrier density n of our material. The results are shown in Fig. 2(c). The sign of the ordinary Hall effect indicates electron-like carriers. At temperatures below T_C , when magnetic order is present, we see that n is almost constant and takes a value of $0.47 \times 10^{22} \text{ cm}^{-3}$ at the lowest temperature. This corresponds closely to the density of Co atoms at the $x = 0.2$ stoichiometry, $0.52 \times 10^{22} \text{ cm}^{-3}$, showing that the Co atoms are very effective donors to dope the material n-type, with donors strongly ionised. The carrier density starts to rise rather linearly on warming above T_C .

4 Conclusion To summarise, we have grown sputtered $\text{Fe}_{1-x}\text{Co}_x\text{Si}$ films at $x \approx 0.2$ that, whilst not being phase pure, have magnetotransport properties that are dominated by the majority B20 phase. In particular, the Co

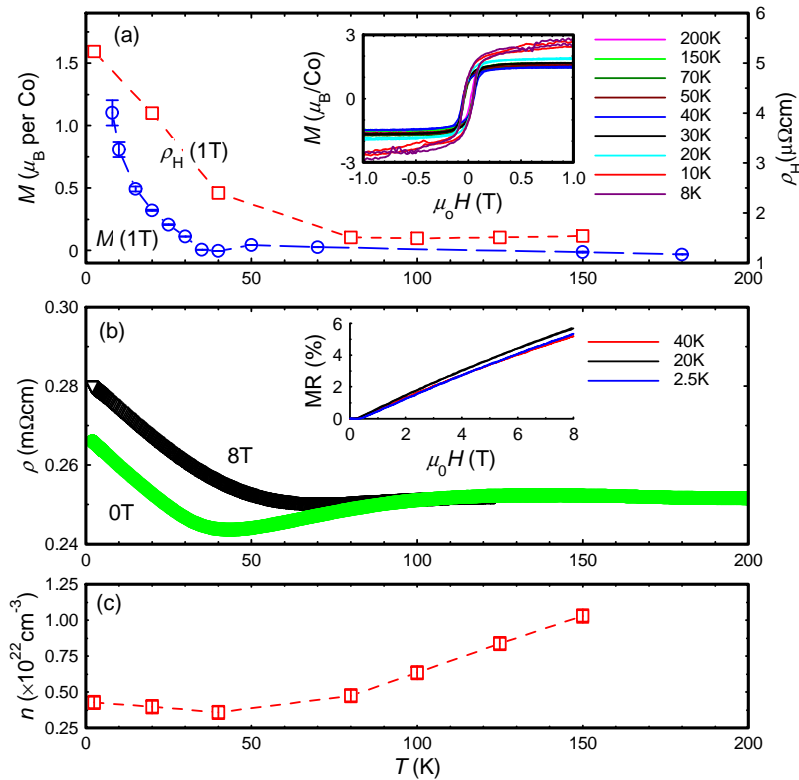


Figure 2 Temperature dependence of magnetic and magnetotransport properties of nominally Fe_{0.8}Co_{0.2}Si thin films. (a) The magnetic moment per Co atom contribution of the ϵ -phase material (the impurity phase background has been subtracted) and the anomalous contribution to the Hall effect, both measured at $\mu_0 H = 1$ T. The curves are similar but not identical. The small discrepancy could be due to the measurements being on different samples, as well as the different field geometry. Inset are VSM hysteresis loops, showing only the ferromagnetic contribution from (Fe,Co) impurity phases at high temperatures, and a more slowly saturating contribution from the ϵ -phase Fe_{0.8}Co_{0.2}Si below $T_C \approx 40$ K. The measurements extended to 2 tesla, showing that all the signals displayed here have saturated. (b) Longitudinal resistivity, with a pronounced minimum at 43 K and a weak maximum at 110 K, characteristic of this material. This minimum is partly washed out at high field, again typical behaviour. Magnetoresistance isotherms are inset, which are very linear in field. (c) (Electron-like) carrier density as determined from the ordinary Hall effect.

atoms act as donors that each contribute close to one carrier each to the electron gas. Magnetometry shows that this phase also possesses almost one μ_B per Co dopant, indicating that in spite of the disorder, a strongly spin-polarised electron gas persists in this silicon-based magnetic semiconductor material. Further growth optimisation, as well as a direct measurement of the carrier spin polarisation of these thin films [17, 18], is desirable.

Acknowledgements This work was partially supported by the (UK) EPSRC. We would like to thank Michael Ward for FIB sample preparation and help with the TEM imaging.

References

- [1] A. I. Al-Sharif, M. Abu-Jafar, and A. Qteish, *J. Phys.:Cond Matt.* **13**, 2807 (2001).
- [2] G. Aeppli and Z. Fisk, *Comments Cond. Matt. Phys.* **16**, 155 (1992).
- [3] V. Jaccarino, G. K. Wertheim, J. H. Wernick, L. R. Walker, and S. Arajs, *Phys. Rev.* **160**, 467 (1967).
- [4] G. Shirane, J. E. Fischer, Y. Endoh, and K. Tajima, *Phys. Rev. Lett.* **59**, 351 (1987).
- [5] T. Jarlborg, *Phys. Rev. B* **51**, 11106 (1995).
- [6] D. Zur, D. Menzel, I. Jursic, J. Schoenes, L. Patthey, M. Neef, K. Doll, and G. Zwirnagl, *Phys. Rev. B* **75**, 165103 (2007).
- [7] M. Klein, D. Zur, D. Menzel, J. Schoenes, K. Doll, J. Röder, and F. Reinert, *Phys. Rev. Lett.* **101**, 046406 (2008).
- [8] N. Manyala, Y. Sidis, J. DiTusa, G. Aeppli, D. Young, and Z. Fisk, *Nat. Mater.* **3**, 255 (2004).
- [9] N. Manyala, Y. Sidis, J. F. DiTusa, G. Aeppli, D. Young, and Z. Fisk, *Nature (London)* **404**, 581 (2000).
- [10] J. Guevara, V. Vildosola, J. Milano, and A. Llois, *Phys. Rev. B* **69**, 184422 (2004).
- [11] S. Bader and S. S. P. Parkin, *Annu. Rev. Cond. Matt. Phys.* **1**, 71 (2010).
- [12] H. von Känel, K. A. Mäder, E. Müller, N. Onda, and H. Siringhaus, *Phys. Rev. B* **45**, 13807 (1992).
- [13] S. Witnachchi, H. Abou Mourad, and P. Mukherjee, *J. Appl. Phys.* **99**, 073710 (2006).
- [14] N. Manyala, B. Ngom, A. Beye, R. Bucher, M. Maaza, J. DiTusa, A. Strydom, A. Forbes, and T. Johnson, *Appl. Phys. Lett.* **94**, 232503 (2009).
- [15] Y. Onose, N. Takeshita, C. Terakura, H. Takagi, and Y. Tokura, *Phys. Rev. B* **72**, 224431 (2005).
- [16] A. L. Schmitt, J. M. Higgins, and S. Jin, *Nano Letters* **8**, 810 (2008).
- [17] R. Meservey and P. M. Tedrow, *Phys. Rep.* **238**, 173 (1994).
- [18] R. J. Soulen, J. M. Byers, M. S. Osofsky, B. Nadgorny, T. Ambrose, S. F. Cheng, P. R. Broussard, C. T. Tanaka, J. Nowak, J. S. Moodera, A. Barry, and J. M. D. Coey, *Science* **282**, 85 (1998).